# Capillary collapse of unsaturated granular soils: experimental investigation and microscale insights

*Nicole* Hüsener[1*] and *Jürgen* Grabe[1]

[1]Institute of Geotechnical Engineering and Construction Management, Hamburg University of Technology (TUHH), Germany

**Abstract.** The capillary collapse is an irreversible volume reduction of partially saturated soils caused by the provision of water at essentially unchanging total vertical stress. Despite extensive research, the processes involved are still not fully understood. Therefore, with the help of a newly developed experimental set-up for CT-based miniature tests presented in this paper, further insights at the micro scale will be gained.

## 1 Introduction

The grain structure of partially saturated soils is mainly stabilized by the so-called capillary cohesion, which results from the matric suction depending on the water content. Due to the increasing dissolution of capillary bridges and the reduction of the matric suction during saturation, the capillary cohesion also decreases significantly. In case of a too low capillary cohesion, the collapse of the microstructure may finally occur. This process, known as capillary collapse, can lead to sudden, substantial settlements in granular soils and has contributed to many damage cases in the past. Although the phenomenon has been known for several decades, the processes involved are still poorly understood. Even though it was recognized early that the microstructure has a crucial influence, there was a lack of suitable investigation methods.

After computed tomography (CT) was originally developed for medical applications, it is increasingly being used in other scientific disciplines. For example, in geotechnical engineering, computed tomography enables the investigation of various processes at the grain scale, thus providing a better understanding of the mechanisms involved. In granular, non-cohesive soils, the capillary collapse typically progresses too fast to be captured in real-time by computed tomography. Due to this limitation, the microscopic studies on this topic are limited. The approach generally underlying CT-based studies of capillary collapse is always based on the aim to induce the collapse in a small-step controlled manner and to reconstruct and follow the processes by CT scans before and after each step.

One disadvantage of computed tomography is that the achievable resolution and quality of the image data drop significantly with increasing specimen size. For the best possible resolution and detailed imaging of the changes occurring during the collapse process, small sample sizes therefore appear advantageous. However, the question arises to what extent these are representative. To circumvent this problem, Bruchon [1] therefore chose a specimen size corresponding to that used in oedometer tests as a common criterion for classifying collapsible soils ($d$ = 70 mm, $h$ = 30 mm). However, the resulting low resolution made it impossible to clearly identify and segment the microscopic structures so that the information obtained on the phase composition is instead based on exploiting the degree of attenuation of the X-rays in the raw images. This approach requires extensive calibration and is sensitive to measurement noise and variations in material density (e.g., due to metal oxides in individual sand grains), since homogeneous attenuation by the individual phases is assumed for the analysis. For this reason, only general tendencies could be derived over the entire specimen. For example, the macroscopic strain distributions were evaluated using volumetric digital image correlation.

In [1] it was also found that the microstructure of the tested material has a double porosity, which collapses as soon as the macropores are saturated by the merging of the capillary bridges between the grain clusters. Furthermore, it was found that the hydrostatic pressure gradient induces vertical heterogeneity of water content and strains, while radial differences could be related to inhomogeneities of initial density or boundary effects. This heterogeneity increases with increasing water content $w$ during the collapse tests. From a water content of about $w$ = 15 % onwards, it was no longer possible to define a representative elementary volume (REV) even with the large sample size used and the initially relatively homogeneous conditions. This indicates that non-uniform microscopic changes occur within the sample during the collapse process, requiring further investigation at the particle scale. It was also observed that a mechanically loaded soil behaved differently during capillary collapse than a soil only subjected to self-weight, but no microscopic studies were performed.

To resolve the changes occurring during the collapse process as best as possible and to image them in detail,

* Corresponding author: nicole.huesener@tuhh.de

the authors in [2] chose a very small cylindrical specimen size with a diameter and initial specimen height of 10 mm. Here, the collapse behavior of a fine and a coarse partially saturated loose pyroclastic sand was investigated. Changes in porosity and water content, tended to be similar for both soils studied, although the increase in water content was more pronounced for the fine sand. Nevertheless, the collapse behavior at the micro level differed significantly due to the different grain size distributions. For example, a radial contraction was initially observed in the fine sand due to the increasing number of capillary bridges before collapsing, which was absent in the coarser sand. However, a possible influence of the specimen size was not considered.

In both studies presented [1, 2], the matric suction was regulated by a hanging water column to trigger the collapse by reducing the matric suction. However, the nonlinear relationship means that even small changes in matric suction can already lead to large settlements, making it difficult to draw conclusions about the microscopic processes from the data. Therefore, to spatially track individual particles or sand grains, the settlements and movements between two scans are likely to be very small, which is not possible with the previously presented approach. Therefore, a new approach was developed, which should allow deeper, more advanced insights and which is presented in this paper. First, the technical set-up of the new test system is introduced. Next, the preparation of the CT experiments by means of preliminary tests in the laboratory is described and important points to be considered during specimen installation are explained. Finally, some exemplary microscopic CT results obtained using the new approach are presented.

## 2 New approach for CT-based collapse tests and microscale insights

To be able to induce the capillary collapse in a more small-step manner than in the already existing CT-based investigations, a new experimental set-up was developed. The set-up essentially consists of a syringe pump controlled by a *Raspberry Pi*, with the help of which individually programmed Python scripts can be used to inject arbitrary volumes of water into the soil specimen at a defined irrigation rate via the specimen bottom. The capillary collapse ultimately results from the sum of the micro-collapses triggered by the individual irrigation steps and can thus be more easily comprehended.

### 2.1 Developed test set-up

The developed set-up is based on the UNSAT-*Pi* 2 system developed by [3] for continuous measurement of transient water retention curves in coarse granular media. The irrigation of small cylindrical soil specimens (diameter of 12 mm, initial specimen height of 12 mm) in a Plexiglas specimen holder is thereby realized via a syringe pump controlled with the help of a *Raspberry Pi* model 3 B+. Due to the lack of hydraulic contact of the pore water pressure sensors at low water contents, these were not used and the system was simplified accordingly (e.g. omission of the A/D-converter).

Since the construction plans for 3D printed syringe pumps available open source have meanwhile been further developed by various researchers and institutions, an optimized version by [4] was used for the experimental set-up. This syringe pump not only allows rapid replacement of the installed syringe, but also provides limit switches. Minor adjustments were only made to the holder for the syringe plunger in order to adapt it optimally to the used 1 ml glass syringe with Luer-Lock connection. The front element was printed twice in order to be able to fix the syringe not only at the rear end and thus provide the pump with more stability.

In addition, a different NEMA stepper motor (model 17HS8401-S) was used. The syringe plunger is driven by the motor via a high quality T8 threaded spindle for 3D printers with a pitch of 1 mm per 360° revolution. The pitch is slightly higher than the 0.8 mm pitch of the M5-threaded spindle used in [3], but finer than the 2 mm pitch proposed in the original construction plans in [4]. However, compared to [3], in the calibration experiments to determine the inner syringe diameter using weight-monitored pump experiments (cf. Fig. 1), there was a significantly lower scatter for the inner diameter determined as a function of flow direction (fill or empty syringe). This behavior could be due to the higher quality of the glass syringe used, which in contrast to the plastic syringe suggested by [3], is designed for multiple applications, as well as a lower backlash. On average of all data, the inner diameters were 4.61004 mm for wetting and 4.61407 mm for drying. Since the collapse tests are based on wetting, this results in an inner cross-sectional area of about 16.692 mm², so the theoretical accuracy of water volume regulation during the wetting test is about $2.608 \times 10^{-3}$ mm³/step. Despite the higher pitch, the smaller cross-sectional area thus results in slightly higher accuracy due to smaller volumes of water moved per step compared to [3].

**Fig. 1.** Calibration set-up for determining the inner syringe diameter using weight-controlled pumping tests.

The Python scripts were modified to set and control the water volumes injected per irrigation step by user inputs instead of the saturation change. During the experiment, the calculated water volume changes are automatically logged in a tabular format. As a result of the user input, the program automatically distinguishes the different initial specimen properties, such as different void ratios and different initial water volumes in the specimen, depending on the material used, i. e. glass beads or model soil. In addition, the irrigation rates can be customized. The two limit switches were also included in the scripts as an additional safety aspect. In this way, for example, the motor stops automatically upon emptying the syringe if the front limit switch is triggered corresponding to a completely emptied syringe.

To avoid additional weak points due to the many jumper wires (e.g. breaking of a PIN or loose contacts), special circuit boards were manufactured instead of the breadboards and protected from further environmental effects with a custom-made housing. The quantity of cables used could thus be reduced to a minimum and the safe transport of the experimental set-up was significantly facilitated. Last but not least, a mini router was integrated into the set-up to be able to control the *Raspberry Pi* remotely via a static IP comfortably without an additionally connected mouse, keyboard and screen. The power supply can be ensured directly via the *Raspberry Pi*. A schematic wiring diagram of all electronic components of the developed experimental set-up is shown in Fig. 2, while Fig. 3 shows a schematic illustration of the entire developed experimental set-up. A photograph of the experimental set-up placed installed in a computed tomography scanner (at Institute of Applied Mechanics of TU Braunschweig, model RX Solutions EasyTom 160-150) can be seen in Fig. 4.

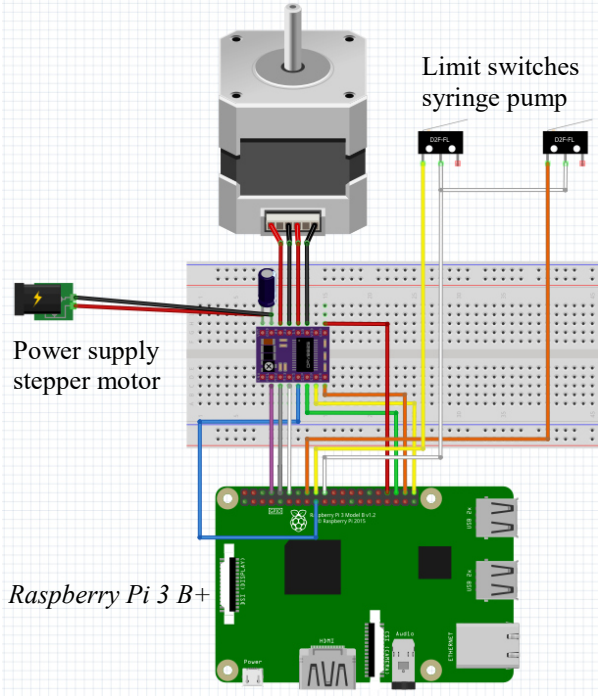


**Fig. 2.** Schematic wiring diagram of all electronic components of the developed experimental set-up.

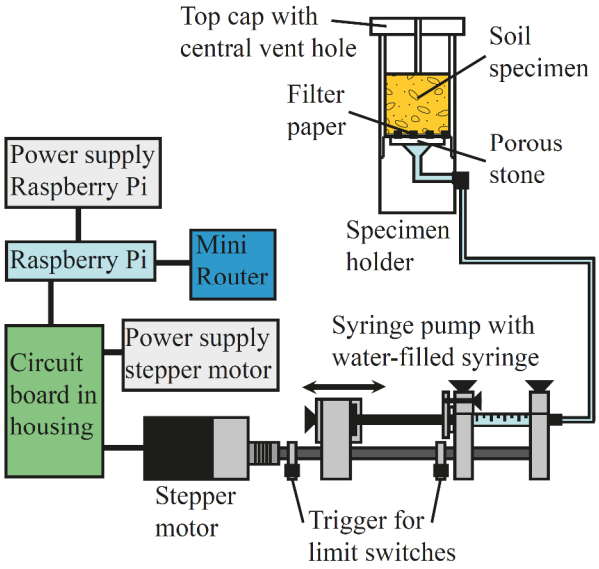


**Fig. 3.** Schematic illustration of the experimental set-up.

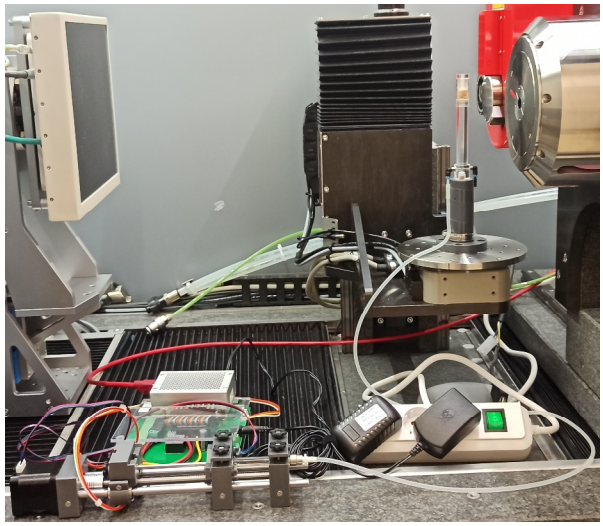

**Fig. 4.** Developed experimental set-up installed in the X-ray CT scanner at Institute of Applied Mechanics of TU Braunschweig. The mini router is connected to the *Raspberry Pi* via the LAN cable, but was placed outside the scan chamber here for organizational reasons.

## 2.2 Specimen preparation and controlled triggering of the small-step capillary collapse

CT-supported miniaturized wetting experiments aim to visualize the processes occurring during capillary collapse at the microscale in an exemplary manner and to analyze them qualitatively and quantitatively, taking into account the effects of various influence factors. For this to succeed, it is particularly important that only very small microscopic changes result from the individual irrigation steps between the CT scans.

Preliminary investigations [1, 5] have shown that there seems to be an almost linear relation between the vertical deformation of the grain skeleton and the degree of saturation [1] or the volume of water supplied [5]. With the help of the new experimental set-up, the capillary collapse is therefore to be induced in a controlled manner, in which only relatively small settlements of the specimen are triggered by small-step

irrigations. In this way, grain movements and changes in the microscopic phase partitioning caused by the irrigation steps can be recorded with the help of CT scans after the individual irrigation steps.

In preparation for the CT tests, it is first necessary to reasonably estimate the water volumes theoretically required to saturate the specimen and to validate them by means of preliminary lab tests. Collapsible soils are often characterized by a particularly loose, metastable bedding. In order to simulate this and to ensure that irrigation itself already leads to visible collapse settlements, a particularly large porosity $n$ is intended at the beginning of the experiment. In partially saturated granular, non-cohesive soils, the porosity can be larger than the maximum void ratio $e_{max}$ determined experimentally on dry soils in the loosest state due to the stabilizing capillary bridges [2, 6]. Without additional loading during the wetting tests, relatively loose bedding is maintained due to air entrapment in the remaining macropores even after saturation at the end of the experiment. The pore volume in loosest state corresponding to $e_{max}$ can therefore be a good initial estimate of the total volume of water to be added. Once the required water volume has been successfully determined, this is divided evenly into a sufficiently large number of small irrigation steps, which are entered later in the python script.

Before installing the specimen, the complete system including the syringe, hoses and the porous filter stone in the specimen holder must be saturated bubble-free with distilled, de-aired water. Attention should be paid to ensure that the syringe is completely filled so that a sufficiently large volume of water is available for the wetting experiments. Similar to [2], a micro-spoon spatula is used for specimen installation of the wet soil material into the specimen holder. Once the specimen is installed, the cap is carefully put in place. A central bore hole ensures atmospheric air pressure in the specimen, while the cap protects the specimen from excessive drying due to evaporation while providing an initially relatively flat specimen surface.

## 3 Selected microscale insights

The miniaturized in situ CT experiments are performed to investigate the triggering microscopic processes. Using the obtained high-resolution image data, the extent and the local course of the resulting settlements as well as morphological changes within the specimen (such as the development of the microscopic phase distribution, local degree of saturation, phase interfaces etc.) can be evaluated by image analysis.

The newly developed approach to induce capillary collapse in a controlled manner in CT-based experiments via a defined, small-step irrigation was tested for the first time in March 2021 during a three-day beamtime measurement period at Institut Laue-Langevin (ILL) [5]. As a special feature, the used NeXT instrument [7] hosts two complementary imaging setups, neutron and X-ray, which can be used in parallel. Here, a total of 5 different experiments were performed. In addition to the Hostun sand already known from [1], a glass bead packing was also investigated. The parallel neutron tomography resulted in a relatively long scan time of about 40 minutes with a voxelsize of about 22.2 µm in the X-ray tomographies.

In the following, some micro-scale results of the third experiment from [5] run at NeXT are shown as an example. The program Avizo was used to analyze the CT image data. Prior to the analysis of the CT data, selected filters were first applied as part of the preprocessing to reduce noise and improve contrast. The segmentation was performed histogram-based. This involves initial phase classification of some voxels based on the intensity and gradient magnitude of these voxels. A marker-seeded watershed transformation is then used to expand the classification so that all voxels become labeled. The result of the preprocessing and segmentation process can be seen in Fig. 5 for an exemplary horizontal slice.

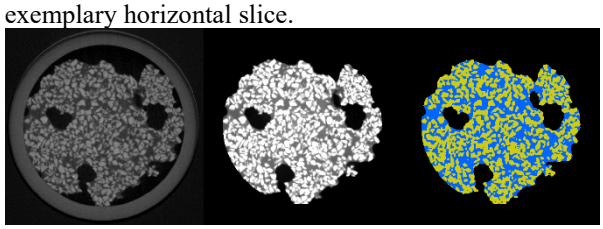

**Fig. 5.** Example of a horizontal slice. Left: raw data, center: after preprocessing, right: segmented data (blue = water phase, yellow = sand phase).

The water supply targeted per irrigation step was 35 µl. A partially saturated soil specimen consisting of 1.592 g of Hostun sand and 0.116 g of water, corresponding to a water content of 7.29 % following [1], was used. From the analysis of the segmented CT data of the initial condition, slightly different values of 1.487 g sand and 0.141 g water were obtained. This may be due to the fact that, for example, at the specimen bottom, not all sand grains might fall completely into the evaluated specimen volume due to the unevenness of the filter stone. For the water volume, where rather low values would have been expected due to evaporation, there might be segmentation errors due to the partial volume effect. An initial sample height of about 13.97 mm (determined with the help of the CT data) resulted in a porosity of about 57%, which is also comparable to the initial conditions of the investigations presented in [1].

Since there were technical problems with the data acquisition in the eighth step, only the results of the initial condition (step 0), the first 7 irrigation steps and step 9 are shown. It should be noted that the hydraulic contact within the sample holder below the filter stone was partially ruptured temporarily. This is presumably due to undesired boundary effects of the combination of the water-repellent specimen holder made of Teflon and the highly capillary-active filter stone. In order to be able to assess the extent to which boundary effects due to the specimen confinement affect the results, a square subsample without contact to the confining specimen holder was also examined in addition to the entire specimen. In the following, however, only the results of the entire cylindrical specimen are presented.

In a first step, the development of the phase distribution over the specimen height was investigated. It can be seen that the distribution of the Hostun sand is

already rather heterogeneous at the beginning (cf. Fig. 6). In the largest part of the specimen, the percentages of the solid fraction vary between approx. 30 and 53 % (step 0). During the test, the percentage of sand in the lower half of the sample increases and the inhomogeneity decreases to some extent. For all steps, it can also be seen that the sand proportion quickly drops sharply at the upper end of the specimen. This indicates an uneven specimen surface (non-uniform material distribution), which could have been reduced by using a cap if applicable. The settlements that occur can also already be recognized well in this way.

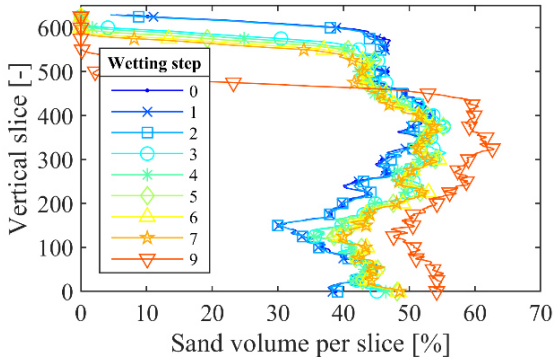


**Fig. 6.** Development of sand volume during CT irrigation test.

When looking at the water phase, it is noticeable that the water concentration at the specimen bottom is significantly increased at the beginning of the experiment (in some cases over 20 % by volume, see Fig. 7). In the rest of the specimen, the fluctuations of the water volume are rather small. Interestingly, the water volumes are initially equalized over the specimen height during the first 2 irrigation steps. While the water volume barely increases in the lower part despite irrigation through the specimen bottom, it increases significantly in the rest of the specimen. However, a reduction in the specimen height does not yet occur at this point (cf. Fig. 8). From the third irrigation step onwards, not only a larger settlement can be observed, but also a significant increase of the water volume over the complete specimen height. In the remaining irrigation steps, the (almost) linear relationship described can be clearly seen (cf. Fig. 8). The water volume increases slightly over the entire specimen height, while at the same time further smaller settlements occur due to the irrigation. Only in step 8 and/or 9 a more severe settlement occurs and a water accumulation forms above the sample.

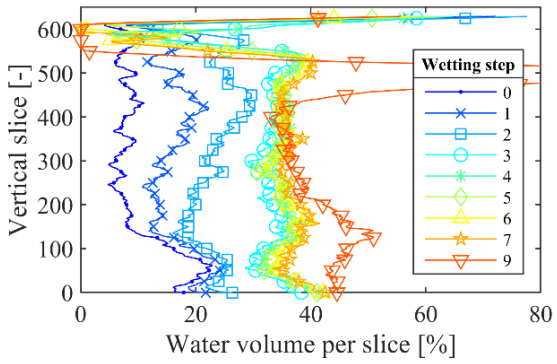


**Fig. 7.** Development of water volume during CT irrigation test.

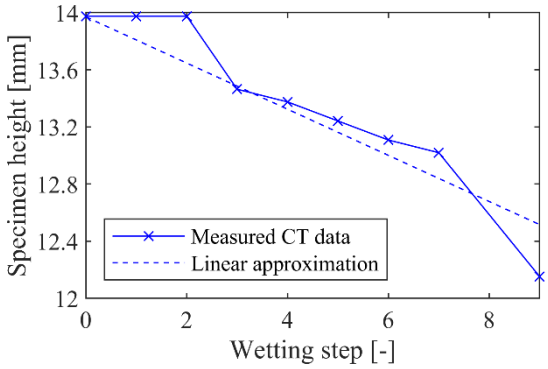


**Fig. 8.** Development of specimen height as a result of the individual irrigation steps.

As expected, the development of the gas phase is mostly opposite to that of the water phase (cf. Fig. 9). At the beginning of the experiment, the air content in the lower part of the sample is lower, whereas during the first two irrigation steps, mainly the air in the pore space of the upper part of the specimen is replaced by water. The settlement that occurs as a result of the third irrigation step can also be seen here by a general decrease in the air volume inside the specimen or an occurring larger air volume above the specimen. The further irrigation steps again lead to a decrease of the air volume, which seems to be slightly more pronounced in the lower part of the specimen. However, despite the accumulation of free water above the specimen observed after step 9, the air is not completely displaced from the specimen. This indicates air entrapment in remaining macropores.

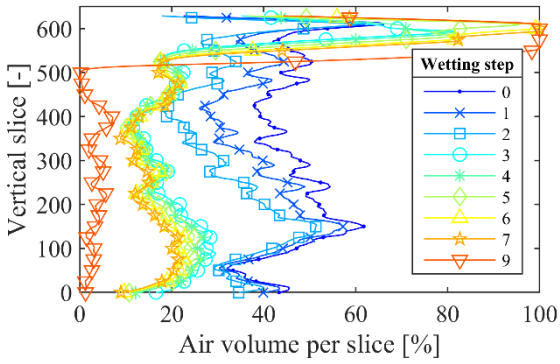


**Fig. 9.** Development of air volume during CT irrigation test.

When considering the derived parameters, such as the porosity or the degree of saturation, the same tendencies were observed overall as already explained for the development of the microscopic phase distribution. The evaluation of the degree of saturation also shows that complete saturation was not achieved despite the fact that the quantities of water added were mathematically sufficient for this and free water even accumulated above the specimen (cf. Fig. 10). Air entrapments in the form of macropores always remained in the sample (cf. Fig. 11). It has been noted in previous studies that repeated irrigation of collapsible soils can also result in further settlement of reduced magnitude [8, 9]. Therefore, the remaining macropores may be partially filled with water during repeated irrigation.

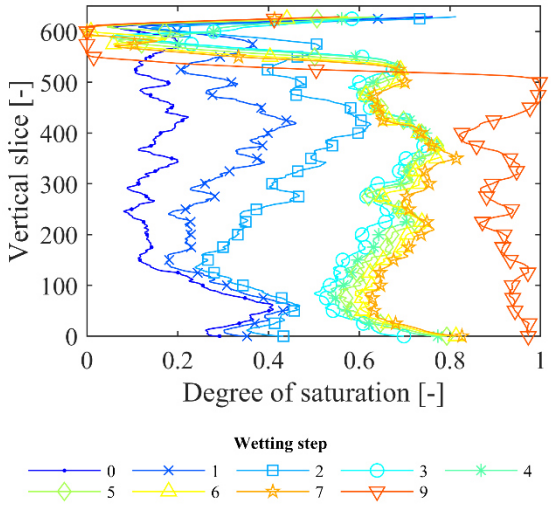


**Fig. 10.** Development of degree of saturation during CT irrigation test.

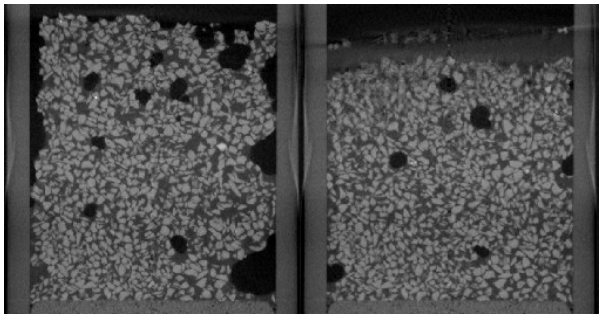

**Fig. 11.** Visible macropores remaining in the sample after irrigation step 7 (left) and step 9 (right), respectively.

## 4 Conclusion and Outlook

Using computed tomography, the newly developed and presented approach of collapse regulation through the small uniform water volumes injected allows new insights into the processes occurring at the micro level. Here, the hypothesis put forward by [1] that heterogeneous microscopic changes occur within the sample during the collapse process as a result of irrigation or saturation could be confirmed overall based on the present evaluated data. However, in order to gain an even deeper understanding of the processes taking place, further data evaluation and experiments are necessary. Particularly noteworthy here are, for example, the analysis of particle movements, the contact angle or the size and localization of individual phase clusters.

For this purpose, extensive CT experiments varying the irrigation rate were carried out at the Institute of Applied Mechanics of TU Braunschweig from 28.11.2022 to 02.12.2022. Here, a significantly better resolution corresponding to a voxel size of only 10 µm could be achieved, allowing higher quality microscopic insights. However, in contrast to the Hostun Sand studied in this paper, three different model soils with approximately the same grain size distribution and increasing degree of complexity due to deviations from the simplest, idealized particle mixture (spherical particles with homogeneous density and uniform size), were examined: a polydisperse glass bead packing, a model soil of natural, randomly shaped sand and a more complex model soil derived from an open-cast mine dump soil containing additional porous lignite particles in addition to the sand particles as an example of a special particle structure.

In addition, further collapse tests of specimens subjected to loading are planned for spring 2023 at the NeXT instrument of the ILL as part of another already allocated two-day measurement period. Here, the combined evaluation of neutron and CT data similar to [10] could allow further interesting conclusions.

The authors greatly acknowledge the funding of the research by the German Research Foundation (Deutsche Forschungsgemeinschaft, DFG) in the framework of Research Training Group GRK 2462: Processes in natural and technical Particle-Fluid-Systems (PintPFS) **[11]** at Hamburg University of Technology (TUHH).

## References

1. J.-F. Bruchon, *Analyse par microtomographie aux rayons X de l'effondrement capillaire dans les matériaux granulaires*. Université Paris-Est. (2004)
2. M. Moscariello, S. Cuomo, S. Salager, Acta Geotechnica **13**, 117-133 (2018)
3. M. Milatz, Acta Geotechnica **15**, 2239–2257 (2020)
4. A. S. Samokhin, Journal of Analytical Chemistry **75**, 416–421 (2020)
5. N. Hüsener, L. Helfen, M. Milatz, A. Tengattini, *Combined X-ray- and neutron-tomography imaging of capillary collapse in unsaturated granular soils*. Institut Laue-Langevin (2021)
6. M. Milatz, N. Hüsener, E. Andò, G. Viggiani, J. Grabe, Acta Geotechnica **16**, 3573–3600 (2021)
7. A. Tengattini, N. Lenoir, E. Andò, B. Giroud, D. Atkins, J. Beaucour, G. Viggiani, Nuclear Instruments and Methods in Physics Research Section A **968**, 163939 (2020)
8. S. Grimmer, *Sackungsprozesse in natürlichen Lockergesteinsfolgen infolge Grundwasser-wiederanstiegs* (2006)
9. M. Milatz, T. Törzs, J. Grabe, Proc. of 7th International Conference on Unsaturated Soils (UNSAT 2018), 255-360 (2018)
10. E. Roubin, E. Andò, S. Roux, Cement and Concrete Composites **104**, 103336 (2019)
11. DFG Research Training Group GRK 2462: Processes in natural and technical Particle FluidSystems (PintPFS), https://gepris.dfg.de/gepris/projekt/390794421?language=en